ACS Sustainable Chemistry & Engineering

Research Article

pubs.acs.org/journal/ascecg

Liquefied-Wood-Based Polyurethane–Nanosilica Hybrid Coatings and Hydrophobization by Self-Assembled Monolayers of Orthotrichlorosilane (OTS)

Anuj Kumar,[*,†,∥,⊥] Marko Petrič,[‡,⊥] Borut Kričej,[‡] Jure Žigon,[‡] Jan Tywoniak,[†,∥] Petr Hajek,[†,∥] Andrijana Sever Škapin,[§] and Matjaž Pavlič[‡]

[†]Czech Technical University in Prague, Faculty of Civil Engineering, Department of Building Structures, Thákurova 7, 166 29 Praha 6, Czech Republic

[‡]University of Ljubljana, Biotechnical Faculty, Department of Wood Science and Technology, Jamnikarjeva, 101, 1000 Ljubljana, Slovenia

[§]Slovenian National Building and Civil Engineering Institute, Dimičeva 12, SI-1000 Ljubljana, Slovenia

[∥]University Centre for Energy Efficient Buildings of Technical University in Prague, Třinecká 1024, 273 43 Buštěhrad, Czech Republic

Supporting Information

ABSTRACT: We have produced hybrid liquefied-wood-based polyurethane (LW-PU) and LW-PU/nanosilica hybrid coatings for wood substrates. The prepared hybrid polyurethane coatings were hydrophobized by self-assembled monolayers of orthotrichlorosilane (OTS) via a sol–gel dipping process. The nanosilica addition into the LW-PU system enhanced the physical properties of coatings like surface hardness and stability toward cold liquids. The OTS hydrophobized coatings were characterized by Fourier transforms infrared spectroscopy (FTIR), scanning electron microscopy (SEM), energy dispersive spectroscopy (EDS), and thermogravimetric analysis (TGA). The surface became hydrophobic as the contact angle (CA) for the water droplet on a modified hybrid coating was ∼115° and very stable. The FTIR, SEM, and EDS analysis confirmed the formation of OTS monolayers on hybrid coatings.

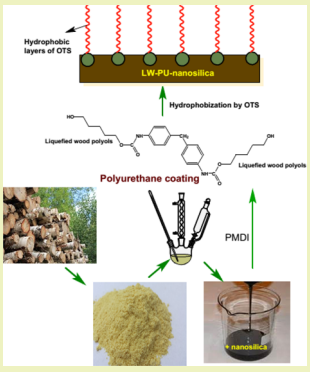

KEYWORDS: *hydrophobic effect, nanoparticles, renewable resources, self-assembly*

INTRODUCTION

Commercial polyols and polyurethanes (PUs) are primarily produced from petrochemical derivatives. Recently, concerns over the depletion of fossil resources have spurred extensive interest in the developing biobased polyols and PUs from renewable resources.[1−3] The biobased polyols for the preparations of PUs have been[1] derived from various hydroxyl-containing renewable biomass resources such as vegetable oils[4,5] and lignocellulosic biomass.[1−3,6−10]

Lignocellulosic biomasses such as wood and agricultural crop residues are considered to be the most abundant renewable biomass. The lignocellulosic biomass mainly consists of cellulose (30−35%), hemicellulose (15−35%), and lignin (20−35%).[11] All of these are highly functionalized materials rich in hydroxyl groups making them promising feedstock to produce various biobased polymers. The liquefaction of woody biomass is usually conducted at elevated temperature (150−250 °C) under atmospheric pressure using polyethylene glycol (PEG), glycerol, or other polyols as liquefaction solvents with an acid- or base-catalyzed reaction.[2,8,9] The produced polyols, which are rich in hydroxyl groups, can be directly used to prepare various PUs for such applications as adhesives,[12] films,[2,7−9] and foams.[13,14]

Organic–inorganic hybrid materials prepared by the sol–gel approach represent a growing and attractive area of nanoengineered materials because of their promise to provide specific peculiarity and multifunctional alternatives to conventional filled plastics.[14] There are numerous reports on silane-treated PU coatings. It is known that the resistance of coatings to water can be improved also by treatment of resins or formulations with silanes,[15] Zhai et al.[16] observed that PU end-capped by alkoxysilane (tetraethyl orthosilicate) via a sol–gel process increased the water contact angle and water resistance of coating films.

Fu et al.[15] found that biobased PU prepared from castor oil modified with a silane (mercaptopropyl trimethoxysilane) exhibited reduced surface energy and, moreover, better mechanical and thermal properties. It is also known that silane–urethane hybrid cross-linkers can improve the mechan-

Received: July 20, 2015
Revised: September 11, 2015
Published: September 14, 2015

DOI: 10.1021/acssuschemeng.5b00723
ACS Sustainable Chem. Eng. 2015, 3, 2533−2541

ical properties of PU films.[17] Just recently Mori[18] published a paper on adding of tetraethoxysilane into liquefied-wood-derived polyurethane. Si was introduced in PU at a molecular level, while maintaining the urethane structure. The mechanical strength of the material was improved.

The main goal of the present work is to develop biorenewable liquefied-wood-based polyurethane−silica nanocomposite coating films at room temperature with enhanced surface properties. Initially, liquefied wood was prepared from black poplar, and polymeric methylene diphenyl diisocyanate (PMDI) was used as a hardener to prepare polyurethanes. Silica nanoparticles in various concentrations were added into liquefied wood before mixing with PMDI. After curing of the obtained liquefied wood (LW)−polyurethane (PU) hybrid coating on wood substrate, wettability of the hybrid coating system was improved by octadecyltrichlorosilane (OTS). The obtained nanocomposite films were characterized for understanding their structural, thermal, surface, and morphological properties.

RESULTS AND DISCUSSION

Chemical Properties of LW-PU and Hybrids Coatings. Analyses of the FT-IR spectra of the LW-PU films were performed after 7 days of curing of the films. The spectra obtained with the LW-PUs and hybrids are shown in Figure 1.

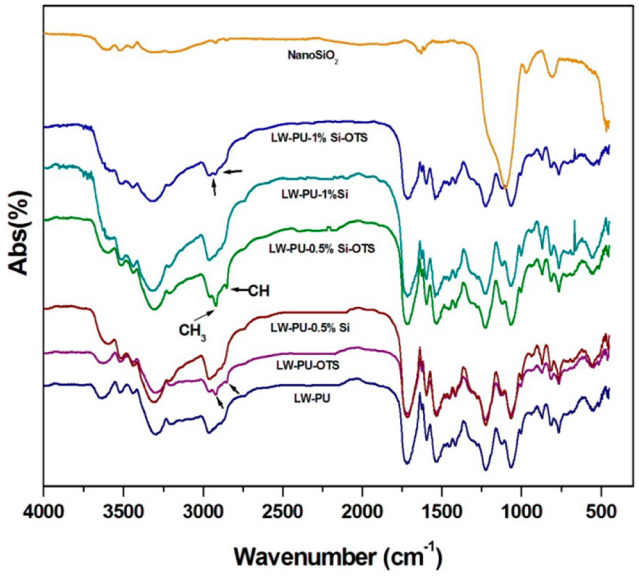

Figure 1. FTIR spectra of LW-PU and hybrid coatings.

From the spectra, it seems that the −NCO groups of the poly isocyanate components were almost completely consumed during the formation urethane bonds. Namely, the band at around 2270 cm^{-1}, representing the asymmetrical stretching vibration of the -NCO group, was not observed.[2]

The absorption band at 1707 cm^{-1} was assigned to carbonyl groups (C═O) initially present in LW and hydrogen-bonded carbonyl groups[19,20] in urethane bonds, resulting from the reaction between hydroxyl groups in LW and the isocyanate hardener. The absorption bands at 3297, 1532, and 1216 cm^{-1}, assigned to the stretching of N−H, bending of N−H with stretching of C−O−N (amide II),[21] and stretching of C−N with bending of N−H (amide III), respectively, were also characteristic of urethane linkages.[22,23] The formation of urea linkages was not seen. The bands characteristic of urea were not observed: 1650 cm^{-1} to 1620 cm^{-1} (amide I), 1580 cm^{-1} to 1550 cm^{-1} (amide II), and 1240 to 1220 cm^{-1} (amide III).[22]

After the OTS treatment, LW-PU coating hybrids were formed. The FTIR spectra of all types of LW-PU hybrids OTS-modified LW-PU coating surfaces, showing numerous OTS assignments, including the $_{\nu a}(CH_2)$ band (~2920 cm^{-1}), the $_{\nu s}(CH_2)$ band (~2850 cm^{-1}), and the $_{\nu a}(CH_3)$ band (~2960 cm^{-1}). The $_{\nu s}(CH_3)$ vibration (~2870 cm^{-1}) is observed as a shoulder on the $_{\nu s}(CH_2)$ band, whereas the $_{\nu a}(CH_2)$ band shape is complicated due to overlapping contributions from broad Fermi resonance bands.[24,25] (Table 1)

The main phenomenon of OTS self-assembled monolayers formation or deposition is well described by Parikh et al.[26] and Bourlinos et al.[27] It is consisting of two-step process consisting of hydrolysis and condensation (see the Figure 2). The amphiphile species (hydrophobic tail in OTS molecules) are first formed in situ by precursor hydrolysis, which in a second step self-assemble, to organize ultimately into a solid cross-linked meso-structure by Si−O−Si condensation. Most likely, in LW-PU coating system, the OTS was hydrolyzed with free −OH groups and formed layered *n*-alkylsiloxane (PODS) gels and polymerized together to form OTS SAM on the LW-PU coating surfaces.[28,29]

The absorption bands at 3450 and 2970 cm^{-1} could be assigned to −OH in the cured films.[2,3] Some hydroxyl groups could have remained unreacted in the films, perhaps because of steric hindrances in the compounds of liquefied wood.[2] Interestingly, the free OH absorption bands are still present after the OTS modifications in the FTIR spectra. Presumably, the hydrogen bonded water bands for the less-well-ordered silane layers, are a consequence of direct interactions with the

Table 1. Chemical Bond Formation Details

chemical assignments	wavenumber (cm^{-1})					
	LW-PU	LW-PU-OTS	LW-PU-0.5% Si	LW-PU-0.5% Si-OTS	LW-PU-1% Si	LW-PU-1% Si-OTS
C═O (carbonyl group) initially present in LW and hydrogen bonded carbonyl groups in urethane bonds[19,20]	1716	1716	1717	1716	1716	1716
N−H stretching[21]	3302	3310	3310	3311	3318	3317
bending of N−H with stretching of C−O−N (amide II[21])	1535	1535	1535	1527	1535	1527
stretching of C−N with bending of N−H (amide III)[22,23]	1223	1223	1223	1223	1223	1223
O−H stretch in LW-PU films[2]	2959	2959	2959	-	2959	2959
C−H stretching region of OTS with two strongest bands that are associated with terminal methyl group (~2870 cm^{-1}) mainly the CH_3 symmetric stretch and its Fermi resonance (~2935 cm^{-1})[24,25]	-	2852, 2924	-	2854, 2923	-	2914, 2955

DOI: 10.1021/acssuschemeng.5b00723
ACS Sustainable Chem. Eng. 2015, 3, 2533−2541

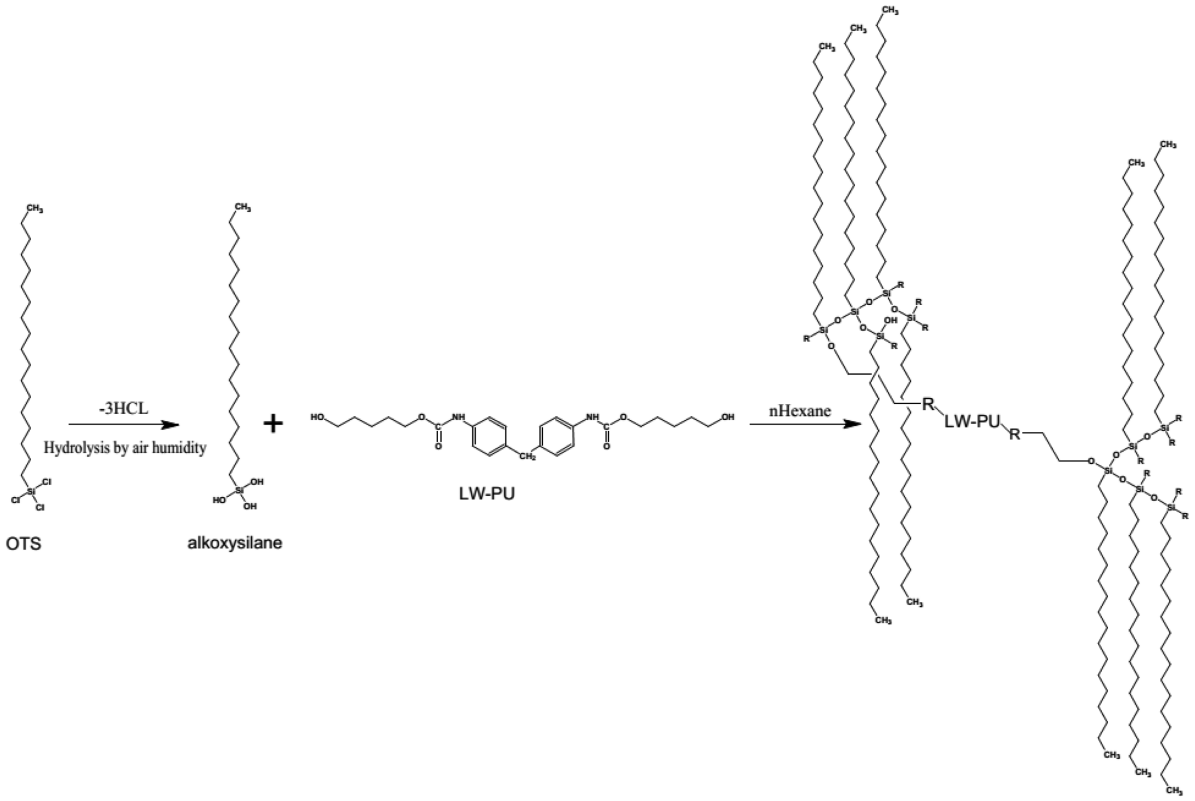

Figure 2. Reaction mechanisms of OTS modification on polyurethane coatings.

underlying fused silica substrate which is made accessible by defects in the hydrophobic monolayer.[30,31]

Table 2 shows the EDS analysis results of hybrid coatings and OTS hydrophobized coatings. The LW-PU coating mainly shows the presence of C, N, and O; this coating was made of liquefied wood and PMDI both containing these elements. Similarly, the LW-PU nanosilica loaded samples show C, O, and N compounds but due to the addition of nanosilica, Si was also evidenced in the system. After the OTS monolayers deposition on hybrid coatings the Si atomic weight percentage was increased (see Figure S1). OTS is an amphiphilic molecule consisting of a long-chain alkyl group ($C_{18}H_{37}-$) and a polar headgroup ($SiCl_3-$).[26,27] It is believed the evaporated Cl compounds form the OTS surface treated surface during hydrolysis, and this is why the presence of Cl was not exhibited by the EDX analysis.

Table 2. EDS's Analysis Results for Hybrids Coating

coating	C	N	O	Si
LW-PU	37.33	32.09	30.58	
LW-PU-OTS	40.06	32.12	27.45	0.37
LW-PU-0.5%Si	40.47	31.02	28.40	0.11
LW-PU-0.5%Si-OTS	43.18	30.85	25.46	0.51
LW-PU-1%Si	41.70	32.34	25.59	0.38
LW-PU-1% Si-OTS	41.10	29.32	28.73	0.85

Physical and Resistance Properties of LW-PU and Hybrid Coatings. The results of the König pendulum hardness test are shown in Figure 3. It can be seen that addition of nanosilica into LW-PU coating slightly increases its hardness; this increase was more evident when a higher amount of nanosilica (1% vs 0.5%) was added. Such a result could be expected, because it is known that addition of nanosilica into PU coatings may increase hardness of the PU films.[32,33] However, it was also reported that the addition of nanosilica may cause a decrease of film hardness.[34,35] The proposed reason for such behavior was formation of nanoparticle aggregates above certain concentration of nanoparticles.[34] On the basis of these reports, one may assume that in our case, aggregates (or agglomerates) of nanosilica were not forms, as indicated by the damping hardness increase. Further on, OTS treatment of the LW-PU coating resulted in much higher hardness increase, which was the most prominent when also nanosilica was present in the films.

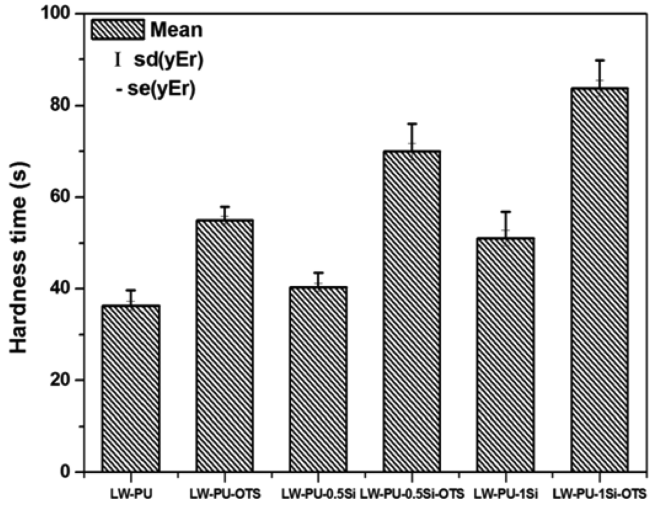

Figure 3. König pendulum hardness of LW-PU and hybrid coatings.

DOI: 10.1021/acssuschemeng.5b00723
ACS Sustainable Chem. Eng. 2015, 3, 2533−2541

Table 3. Mechanical and Resistance to Cold Liquids Properties of LW-PU Hybrid Coatings

composition of LW-PU	adhesion		resistance to scratching (N)	resistance to cold liquids	
	MPa (std dev)	type of failure[a]		water (1 h)	alcohol 48% (1 h)
LW-PU	2.16 (0.20)	C	1	2	2
LW-PU-OTS	-	-	3	4	3
LW-PU-0.5%Si	2.21 (0.31)	C	2	3	2
LW-PU-0.5%Si-OTS	-	-	3	4	3
LW-PU-1%Si	2.27 (0.18)	C	2	3	2
LW-PU-1% Si-OTS	-	-	3	4	3

[a]C Cohesive-type failure - the substrate was broken during the test. Due to OTS treatment, the coated surface became very hydrophobic, and adhesive was not glued over it.

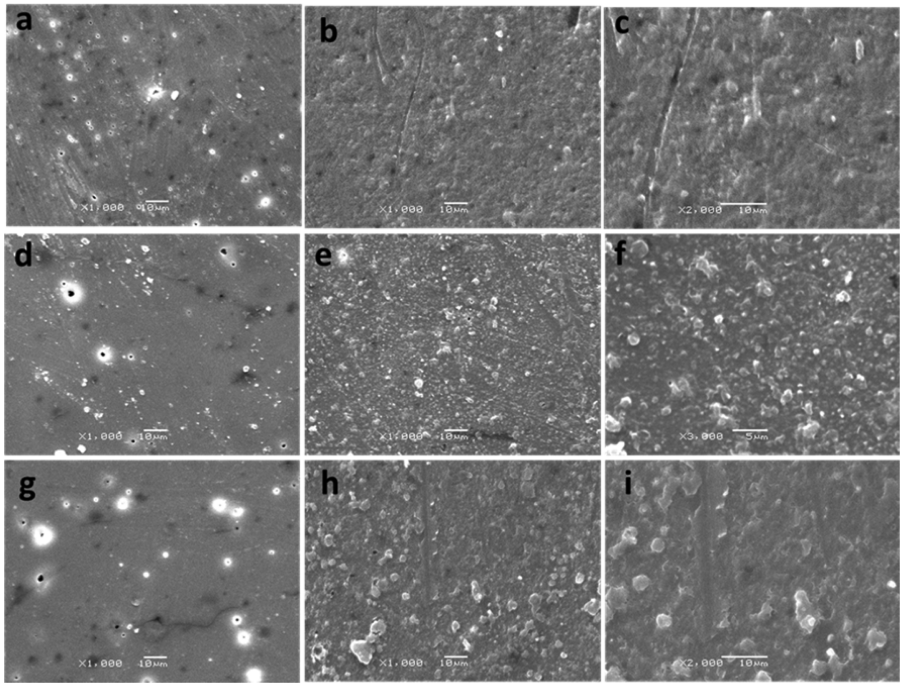

Figure 4. SEM images of hybrid coatings (a) LW-PU; (b, c) LW-PU-OTS; (d) LW-PU-0.5% Si; (e, f) LW-PU-0.5% Si-OTS; (g) LW-PU-1% Si; and (h, i) LW-PU-1% Si-OTS.

Due to OTS treatment, the coated surface became very hydrophobic and even two-pack epoxy adhesive was not able to glue the dollies on the OTS treated LW-PU films. In other cases, we could determine the tensile strength, but the problem was that we obtained cohesive failure of the wood in all cases (Table 3). A possible explanation for the observed fracture could lie in the low tensile strength of the spruce wood (especially early wood), or it could be explained as it was by Ugovsek et al.,[36] who studied the wood bond line when liquefied wood was used as an adhesive. They proposed at least partial in situ liquefaction of the substrate after application of the liquefied-wood-based adhesive, in the period until the end of the curing process, forming a weak boundary layer of delignified wood cells. Nevertheless, we can conclude that the addition of nanosilica is not making the situation worse; the tensile strength is even a bit higher.

The resistance of the films to scratching was rather low (Table 3). The LW-PU coating film cracked already at the load of 1 N. However, as it was in case of coating hardness, the addition of nanosilica into LW-PU coating also slightly increased the resistance to scratching (from 1 to 2 N), but this increase was not dependent on the added amount of nanosilica. As proposed by Wang et al.,[32] improved mechanical properties, due to addition of nanosilica, could be explained by the increase of the cross-linking density of the polymer. However, at higher concentration, resistance could even decrease because of poor interaction between matrix polymer and dispersed phase of nanosilica.[35] It is interesting that OTS treatment of pure LW-PU or with addition of nanosilica (0.5% or 1%) is also increasing the resistance to scratching even more evident (from 1 or 2 N to 3 N). Fu et al.[15] found that biobased PU prepared from castor oil modified with a silane (mercaptopropyl trimethoxysilane) exhibited reduced surface energy and, moreover, better mechanical and thermal properties. It is also known that silane−urethane hybrid cross-linkers can improve the mechanical properties of PU films.[17]

Resistance to cold liquids is for a coating of a great importance, but because we already established in our previous researches that resistance to water and alcohol is a week point of LW-based PU coatings,[2,9] we focused only on these two liquids (Table 2). The addition of nanosilica did improve the resistance to water (the grade improved from 2 to 3), but it did not have any effect on resistance to alcohol. On the other hand, OTS treatment significantly improved the resistance to water (the grade improved from 2 or 3 to 4) and also the resistance to alcohol (the grade improved from 2 to 3), independent of

DOI: 10.1021/acssuschemeng.5b00723
ACS Sustainable Chem. Eng. 2015, 3, 2533−2541

whether the coating nanosilica was already added. Research on similar LW-based coating systems suggested that the sensitivity of the films to polar solvents (water and ethanol) arose from the presence of some residual hydroxyl groups in the film network structure.[2] This might be the reason also in our case, because the ratio between isocyanate and hydroxyl groups −NCO/OH of 0.5 was rather low. Similarly, low resistance to water was proposed to be the consequence of a low cross-linking rate in self-cross-linked LW-based coatings.[9] On the other hand, this would also explain higher resistance to water of nanosilica included and OTS treated coatings. As established by Wang et al.,[32] the addition of nanosilica into a coating is increasing the cross-linking density of the polymer. Furthermore, we can connect a good resistance to water (grade 4) of the OTS-treated coatings with the hydrophobic surface of films after the treatment.

Morphological Properties of LW-PU and Hybrid Coating Systems. Figure 4 shows morphologies of cured LW-PU hybrids coatings on a wood substrate. The LW-PU and LW-PU with nanosilica show smooth and flat morphology with some air bubbles trapped in the system (panels a, d, and g of Figure 4). The dispersion of nanosilica looks uniform in the SEM images, and no agglomeration of nanosilica particles appears. This observation supports the influence of nanosilica particles on the hardness of coating, which was increased (see the previous chapter), in contrast to possible hardness decrease due to nanoparticles aggregates, as described in the literature.[38,39] After hydrophobization by self-assembled layers of OTS, the surface morphologies were significantly changed. The coating surface was uniformly covered by the self-assembled layers of OTS: the SEM images reveal a striated surface texture, suggesting the presence of lamellae of layer deposition the surfaces (see panels b, e, and h of Figure 4). Similar type of results was reported in literature.[27]

The surface coverage resulting from the expected silanization reaction involving OTS and hydroxylic substrates,[37] was the main reason to choose the low−NCO/OH ratio of 0.5 during preparation of PU coatings from liquefied wood. Self-assembled monolayers (SAMs) are ordered molecular assemblies that are formed spontaneously by the absorption to a surface with a specific affinity of its headgroup to the substrate.[37] In the present study, the formation of OTS layers is clearly observed on the OTS treated surfaces of LW-PU coating (Figure 4). The hydrophobic tails of these OTS layers on the surfaces make the surface coating hydrophobic.

Thermal Properties of LW-PU and Hybrid Coating Systems. TGA measurements were performed to evaluate the thermal stability of the LW-PU and nanocomposites, and the results are presented in Figure 5a and in Table 4. The LW-PU coatings show three main thermal degradation phenomena during thermolysis under N_2: in the 100−150 °C range, in the 150−300 °C range, and at temperatures higher than 300 °C (Figure 4a). The first weight loss event accounts for about 15% of mass reduction in liquefied wood and may be ascribed to evaporation of trapped solvents and water. The second degradation step yields another 15% mass loss and may be associated with the breaking of α- and β-aryl-alkyl-ether linkages, aliphatic chains, and decarboxylation reactions.[3] Finally, the third broad and sharp mass loss event (above 300 °C) may be related to the rupture of carbon−carbon linkages between liquefied wood and urethane linkages, primarily by the decomposition of isocyanates in urethane polymer.[38,39]

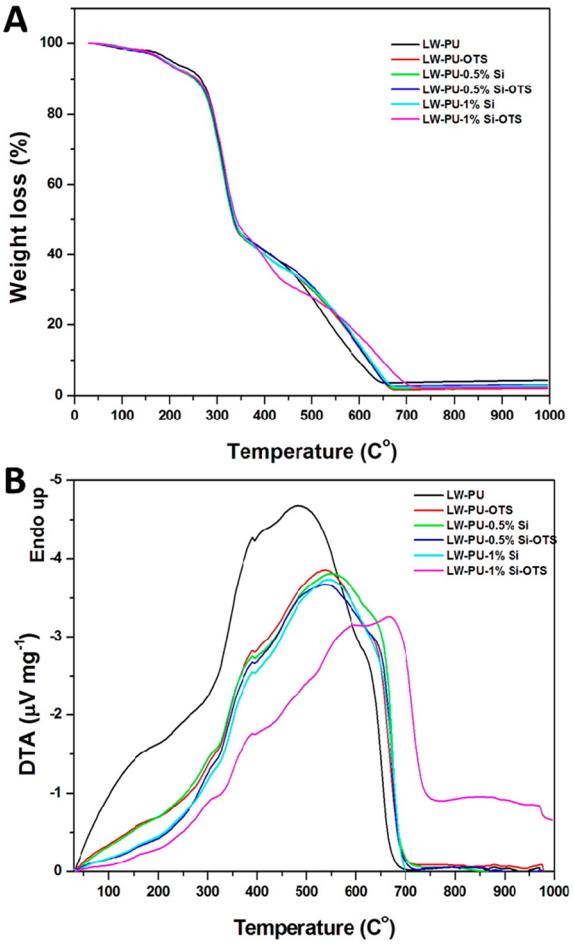

Figure 5. (a) TGA curves and (b) DTA curves of LW-PU hybrid coatings.

Nanosilica-loaded LW-PU and OTS-modified LW-PU samples showed a similar weight loss along the accelerated temperatures, as shown in Table 4. The residue weight percentages at 600 °C, increased with the nanosilica weight percentage. Further, after OTS treatment, the residue weight percentages increased due to the deposition of silica in self-assembled layers of OTS (Table 3).

Figure 5b shows approximately two distinct regions of weight loss for every DTA plot of LW-PU samples. The first part of the degradation correlates with the diisocyanate component, whereas the second peak correlates with the degradation of cellulose in wood and plasticizer.[39]

The main degradation temperature peaks of LW-PU samples in the DTA are between 350 and 550 °C. This can be explained from two aspects: the diisocyanate mixing into liquefied wood and the cross-linkages thus formed between wood components and diiocyanate causing the increase of the starting degradation temperature of wood.[39] The LW-PU-1% Si-OTS sample shows another DTA peak at higher temperature ∼667 °C (Table 4 and Figure 5b). This may be due to the formation of stable covalent bonds Si−O−Si between nanosilica and silane present in the OTS layers.[40]

Hydrophobization of LW-PU Hybrid Systems. As reported,[9] liquefied-wood-based polyurethanes are less stable in humid conditions; therefore, in this was another reason that we modified the LW-PU coating surfaces by deposition of layers of OTS. The initial apparent (none of the surfaces

DOI: 10.1021/acssuschemeng.5b00723
ACS Sustainable Chem. Eng. 2015, 3, 2533−2541

Table 4. Thermal Degradation Temperatures at 10% ($T_{10\%}$), 25% ($T_{25\%}$), and 50% ($T_{50\%}$) Mass Loss, Char Residue at 600 °C (R650) and Maximum Mass Loss Derivative Temperature Analysis ($T_{DTA\ max}$) for Liquedfied-Wood-Based PU Nanocomposites As Obtained from TGA Measurements under N_2

coatings	$T_{10\%}$ [C°]	$T_{25\%}$ [C°]	$T_{50\%}$ [C°]	R_{600} [%]	$T_{DTA\ max}$ [C°]
LW-PU	248.5	296.5	333	9.45	483
LW-PU-OTS	258.5	302	326	12.5	534
LW-PU-0.5%Si	248.5	294	333	11.42	548
LW-PU-0.5%Si-OTS	261	303	335	14.32	552
LW-PU-1%Si	265	296	335	13.02	549
LW-PU-1% Si-OTS	272.5	301	338	17.45	562 and 667

studied could be considered as an ideal one, so the term "apparent contact angle" should be used) contact angles of distilled water on LW-PU and LW-PU-0.5% Si, measured 1 s after the dispenser tip detachment from the drop, had the values of around 74° and 76°, respectively. Somewhat lower initial water contact angle of 66° was observed on surfaces of LW-PU-1% Si. The lower contact angle in this case could be tentatively the result of a bit higher surface roughness due to higher nanosilica loading (1%), although the presumed surface roughness cannot be clearly seen in Figure 4g. It is well-known that contact angles of water can be decreased when surface roughness of hydrophilic surfaces is increased.[40]

The other possible reason for this decrease could simply be the increased hydrophilic character of the surface because of the higher content of SiO_2. Contact angle of water on surfaces of LW-PU, LW-PU-0.5% Si, and LW-PU-1% Si decreased within 60 s of contact angle measurements (Figure 6), exhibiting

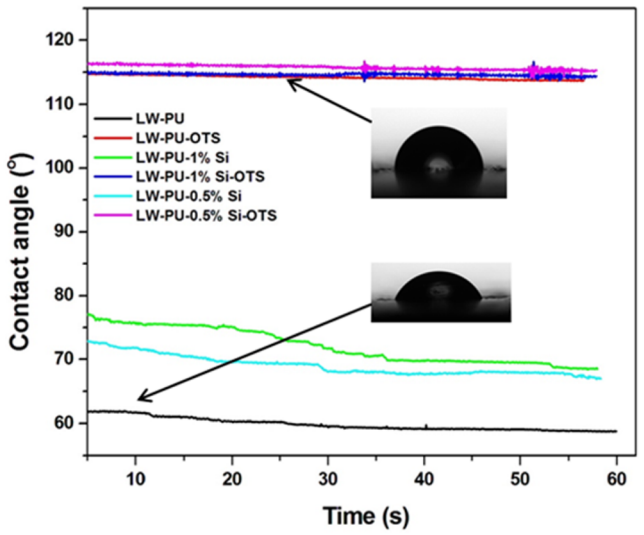

Figure 6. Contact angles of water, depending on time after drop deposition, on surface LW-PU hybrid coatings.

interactions with the substrates, presumably penetration of water into LW-PU or LW-PU-Si films. After the treatment with OTS, the contact angles of water increased up to the average value of 115° at LW-PU-1%Si-OTS, as measured 1 s after detachment of the dispenser tip. Importantly, contact angles of water on the OTS treated surfaces remained stable and did not change with time, indicating the absence of penetration of water into the films (Figure 6).

The two most likely reasons for hydrophobization of the surfaces are (a) the presence of hydrophobic alkyl groups in self-assembled layers of OTS and (b) OTS increased surface roughness of the LW-PU coatings (panels c, f, i of Figure 4). When the roughness of the hydrophobic surface is increased, usually also its hydrophobicity is increased.[41] Similarly, a poly(vinyl alcohol) (PVA)/SiO_2-based very stable and superhydrophobic composite coating on wooden substrates was reported where the PVA/SiO_2 coatings were also modified with OTS.[41] In another study, epoxy/nanosilica coatings was modified by OTS treatment to make them superhydrophobic.[42]

Analysis of volumes of water drops showed some differences in volumes 1 s after the dispenser tip detachment and after 60 s. Although standard deviations are high (see Figure 7), there are

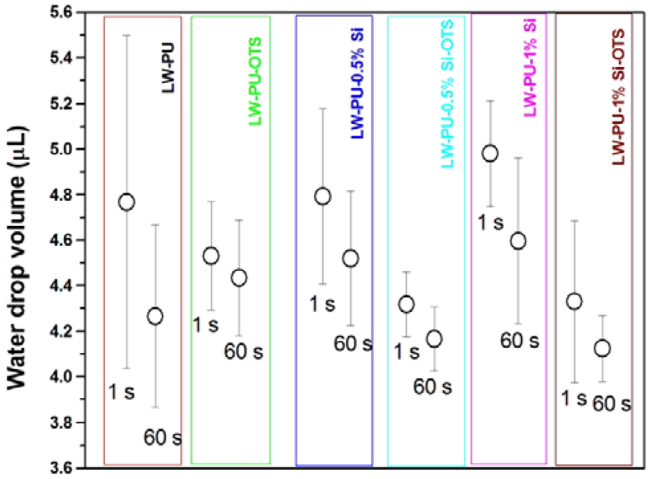

Figure 7. Volume of water droplets on the coating surfaces as a function of time.

indications that the decrease of volume was quite lower on the substrates treated with OTS than on the substrates without OTS (LW-PU and LW-PU-Si). This indicates that there was some penetration of water during first 60 s after deposition into the films without OTS and that OTS prevents penetration of water into liquefied-wood-based coatings. This observation corresponds well with the observed increased hydrophobicity of the OTS-treated coatings, and the present results are in good agreement with the phenomenon of water drop volume change with time about the hydrophobicity surfaces mentioned in literature.[43]

CONCLUSIONS

OTS molecules were grafted onto surfaces of polyurethane films made of liquefied wood (LW-PU) and on the films loaded with nanosilica (LW-PU-Si), forming hydrophobic layers, and so new hybrid coatings were prepared. It was found out that the OTS hydrophobized surfaces exhibited much better coating properties, when compared to the properties of LW-PU and

DOI: 10.1021/acssuschemeng.5b00723
ACS Sustainable Chem. Eng. 2015, 3, 2533−2541

LW-PU-Si coatings. The described novel and feasible strategy is suitable for construction of hydrobhobized liquefied-wood-based polyurethane coatings.

EXPERIMENTAL SECTION

Materials. Black poplar (*Populus nigra* L.) wood was ground, sieved using a 0.24 mm screen, and oven-dried at 103 °C for 24 h prior to the liquefaction reaction. PMDI (15.2%) was obtained from Chemcolor (Slovenia). Spruce wood samples and glass plates were used as substrates for coatings. Trichloro(octadecyl)silane (≥90%) and silicon dioxide nanoparticles (15 nm) were purchased from Sigma-Aldrich. Glycerol, PEG #400, sulfuric acid, and *n*-hexane, 95% (Optima) were procured from Fisher scientific.

Preparation of Liquefied Wood. Liquefaction of wood was conducted in a 1 L reactor using a mixture of polyethylene glycol #400 (PEG) at a 9:1 mass ratio as the reactive solvent and sulfuric acid as the catalyst. The wood-to-solvent mass ratio was 1:3, and the catalyst-to-solvent mass ratio was 3:100. Glycerol, PEG #400, sulfuric acid, and wood sawdust were charged into the reactor and refluxed under continuous mechanical stirring for 90 min at 180 °C. After this time, the liquefied mixture was cooled and diluted with a 1,4-dioxane/water mixture (4:1, v/v). The residue from liquefaction was removed by filtration under vacuum through a filter disk (Sartorius 388 grade, 12 to 15 μm particles retention). LW was obtained after evaporation of dioxane and water.

Determination of the Hydroxyl Number and Acid Numbers of LW. The hydroxyl number and acid number of the LW was determined according to the procedure described in the literature.[7,12] The calculated values of hydroxyl number and acid number for LW were 333.57 and 11.16, respectively.

Preparation of Liquefied Wood and Nanosilica Hybrids for Coatings. The nanosilica to LW at mass ratios of 0.5%, and 1%, (based on LW) were prepared by mixing them together using IKA T25 Ultra-Turrax ((dispersing tool S 25 N − 18 G, at revolutions of 6000 min^{-1}) for 10 min each and subsequent ultrasonication treatment to disperse the nanosilica into LW. Homogeneous LW and LW−nanosilica mixtures were used in the preparation of LW-PU coatings. The −NCO/OH molar ratio was fixed 0.5 for all samples. Three different type of LW-PU coatings were prepared: one was control (LW-PU), the second one was prepared with 0.5% silica (LW-PU-0.5% Si), and the third one with 1% silica (LW-PU-1% Si).

LW-PU Coatings Preparations on Wood and Glass Plates. Glass plates were cleaned by using ethanol prior to application of coatings. For different tests, various spruce (*Picea abies* (L.) Karst) samples free from knots and cracks, of straight grain and normal growth rate, were prepared. For coating, radial surfaces were always used. Prior to coating, surfaces were sanded with 180 grit sandpaper, and dust particles were removed as much as possible.

The fixed amounts of LW and isocyanate hardener were mixed to obtain the −NCO/OH molar ratio of 0.5. The manual coating film applicator was used to prepare a uniform layer of LW-based polyurethane coatings on wood and glass plates. The approximately 80 μm (one coat) thick layers were formed on the glass plates and similarly, approximately 80 μm (two coats of 40 μm with 24 h of intermediate drying time) thick film was formed on wood substrates. All films were characterized after 7 days of curing and conditioning at a temperature of (23 ± 2) °C and relative humidity of (50 ± 5) %.

Sol−Gel Surface Modification of LW-PU Nanosilica Hybrid Coating by OTS. The solution (1/100) (v/v) of orthotrichlorosilane (OTS) in *n*-hexane was prepared, and all the samples were dipped in the solution for 2 h to grow the hydrophobic OTS layer on the coating films. After the dipping process, the samples were washed with *n*-hexane to remove the remaining of OTS that was not adhered to the substrate and dried at 60 °C for 2 h. The naming of OTS modified samples is as follows: LW-PU-OTS, LW-PU-0.5% Si-OTS, and LW-PU-1% Si-OTS.

FT-IR Analyses. FT-IR analyses were performed with a PerkinElmer (U.S.A.) Spectrum One FT-IR spectrometer using the horizontal attenuated total reflection (HATR) technique (with a HATR ZnSe 45° flat plate). All of the spectra were recorded at 4 cm^{-1} resolution, and each was the average of 32 scans. The samples were oven-dried at 80 °C for 2 h before the measurements.

Determination of Hardness by the Pendulum Damping Test Method. The hardness of the cured films on glass plates was determined by a König pendulum test according to the method of damped oscillations (EN ISO 1522:2001).[44] The hardness value corresponded to the damping time of the pendulum oscillating on the film surface from 6° to 3°.

Resistance to Scratching. The resistance of the films to scratching was determined according to the standard EN ISO 1518:2000.[45] The scratching needle, with a hard hemispherical tip 1 mm in diameter, was drawn across the surface of the coated test specimen, perpendicular to the grain direction, at a constant speed (30 to 40 $mm{\cdot}s^{-1}$). Scratching was performed on different parts of the test panels, using an increasing load on the scratch needle, until the coating cracked or the scratch was wider than 0.5 mm. The force level in N, which produced such damage, was defined as a critical scratch, exhibiting resistance to scratching.

Adhesion Determined by the Pull-off Test Method. A pull-off test was used to measure the adhesion between PU films and a wood substrate. The procedure described in EN ISO 4624:2003[46] was carried out: aluminum dollies were glued onto the coating film with a two-pack epoxy adhesive. After 24 h of drying under room conditions, the dollies were isolated from the surrounding film with a cutting tool. The adhesion was measured using a DeFelsko(USA) PosiTest AT adhesion tester that applied a tensile load perpendicular to the test surface. The tensile stress in MPa and the type of the failure (adhesive or cohesive) were recorded.

Resistance to Cold Liquids. The resistance to water (distilled water) and to alcohol (48% aqueous solution of ethanol) was determined according to the standard EN 12720:2009.[47] Paper disks (25 mm in diameter, 480 $g{\cdot}m^{-2}$) were dipped into the test liquid (at a temperature of (23 ± 2) °C) for 30 s, then placed onto the coated surface and covered with a standardized glass cup for the test period (1 h). After the test period, the glass cups and paper disks were removed, and after 20 h, the surfaces were cleaned and assessed according to the numerical rating codes defined in the standard (from 1 to 5), where 5 represents the best assessment (no visible damage) and 1 the poorest.

Scanning Electron Microscopy (SEM-EDS) Measurements. Morphology of cured LW-PU films and hybrid coatings on wood substrates was studied by scanning electron microscopy (SEM, JEOL JSM-5500LV, Japan) coupled with Oxford's Energy-dispersive X-ray spectroscopy (EDS), used for elemental analysis or chemical characterization of samples. All

DOI: 10.1021/acssuschemeng.5b00723
ACS Sustainable Chem. Eng. 2015, 3, 2533−2541

surfaces were cleaned with alcohol, in order to remove dust, and then coated with a thin evaporated layer of gold to improve the conductivity prior to analyses.

Determination of Contact Angles of Distilled Water. The Theta (Optical Tensiometer) contact angle goniometer from Biolin Scientific Oy, Espoo - Finland, was used to determine the contact angles of distilled water on surfaces of control and surface finished wood specimens. When the goniometer microscope was focused and adjusted on the image of the drop, it was ensured that the contact angles on each side of the drop were approximately the same. The contact angles were measured by means of computer-aided analysis (OneAttension, Version 2.4 (r4931), Biolin Scientific, Young−Laplace contact angle analysis mode) of shapes of liquid drops, as observed in an optical goniometer and recorded by a digital camera installed in axial extension of the lens.

The drops of about 4−6 μL (the volumes were calculated from images of drops) were applied by means of a dispenser. Image recording was set for 60 s, and the time when contact angles started to be calculated (0 s) was after detachment of the dispenser tip from the drop, which happened approximately 1.30 s after the first contact of the drop with a substrate. The read-outs were taken for 15 pictures for different drops of water, and the arithmetic mean value was reported. The measurements were taken at the constant temperature of 23 °C.

Thermogravimetry Analyses (TGA) and Differential Thermal Analyses (DTA). The thermogravimetric (TG) measurements were performed on a Netzsch STA 409 Instrument from room temperature up to 1000 °C with a heating rate of 15 C° min^{-1}. Samples with an initial mass of around 10−30 mg were placed into Al_2O_3 crucibles. During the measurement, the furnace was purged with an air flow with a rate of 20 mL·min^{-1}. The baseline was automatically subtracted from the measured TGA curve. Differential thermal analysis (DTA) measurements were performed simultaneous along on a Netzsch 409 Instrument.

■ ASSOCIATED CONTENT

Supporting Information

The Supporting Information is available free of charge on the ACS Publications website at DOI: 10.1021/acssuschemeng.5b00723.

EDX analysis curves for all the coating systems (PDF)

■ AUTHOR INFORMATION

Corresponding Author

*E-mails for A.K.: anuj.kumar@fsv.cvut.cz; anuj.saroha@gmail.com. Tel.: +420 224357147. Fax: +420 233339987.

Author Contributions

⊥These authors contributed equally (A.K. and M.P.). The manuscript was written through contributions of all authors. All authors have given approval to the final version of the manuscript.

Notes

The authors declare no competing financial interest.

■ ACKNOWLEDGMENTS

This research work was supported by the European social fund within the framework of realizing the project "Support of intersectoral mobility and quality enhancement of research teams at Czech Technical University in Prague", CZ.1.07/2.3.00/30.0034. Financial support of the Slovenian Research Agency through the research programme P4-0015 "Wood and lignocellulose composites" is also gratefully acknowledged.

■ REFERENCES

(1) Hu, S.; Luo, X.; Li, Y. Polyols and polyurethanes from the liquefaction of lignocellulosic biomass. *ChemSusChem* **2014**, *7*, 66−72.

(2) Cheumani-Yona, A. M.; Budija, F.; Hrastnik, D.; Kutnar, A.; Pavlič, M.; Pori, P.; Tavzes, T.; Petrič, M. Preparation of Two-Component Polyurethane Coatings from Bleached Liquefied Wood. *BioResources* **2015**, *10* (2), 3347−3363.

(3) Griffini, G.; Passoni, V.; Suriano, R.; Levi, M.; Turri, S. Polyurethane Coatings Based on Chemically Unmodified Fractionated Lignin. *ACS Sustainable Chem. Eng.* **2015**, *3* (6), 1145−1154.

(4) Xia, Y.; Larock, R. C. Vegetable oil-based polymeric materials: synthesis, properties, and applications. *Green Chem.* **2010**, *12* (11), 1893−1909.

(5) Zhang, C.; Kessler, M. R. Bio-based Polyurethane Foam Made from Compatible Blends of Vegetable-Oil-based Polyol and Petroleum-based Polyol. *ACS Sustainable Chem. Eng.* **2015**, *3* (4), 743−749.

(6) Pizzi, A. Wood products and green chemistry. *Ann. For. Sci.* **2015**, 1−19.

(7) Hrastnik, D.; Humar, M.; Kričej, B.; Pavlič, M.; Pori, P.; Cheumani Yona, A.M.; Petrič, M. Polyurethane coatings from liquefied wood containing remains of a copper-, chromium-, and boron-based wood preservative. *J. Appl. Polym. Sci.* **2014**, *131* (19), 40865 DOI: 10.1002/app.40865.

(8) Cheumani Yona, A. M.; Budija, F.; Kričej, B.; Kutnar, A.; Pavlič, M.; Pori, P.; Tavzes, C.; Petrič, M. Production of biomaterials from cork: Liquefaction in polyhydric alcohols at moderate temperatures. *Ind. Crops Prod.* **2014**, *54*, 296−301.

(9) Budija, Franc; Tavzes, C.; Zupančič-Kralj, L.; Petrič, P. Self-crosslinking and film formation ability of liquefied black poplar. *Bioresour. Technol.* **2009**, *100* (13), 3316−3323.

(10) Kurimoto, Y.; Takeda, M.; Koizumi, A.; Yamauchi, S.; Doi, S.; Tamura, Y. Mechanical properties of polyurethane films prepared from liquefied wood with polymeric MDI. *Bioresour. Technol.* **2000**, *74* (2), 151−157.

(11) Behrendt, F.; Neubauer, Y.; Oevermann, M.; Wilmes, B.; Zobel, N. Direct liquefaction of biomass. *Chem. Eng. Technol.* **2008**, *31* (5), 667−677.

(12) Kunaver, M.; Medved, S.; Čuk, N.; Jasiukaitytė, E.; Poljanšek, I.; Strnad, T. Application of liquefied wood as a new particle board adhesive system. *Bioresour. Technol.* **2010**, *101* (4), 1361−1368.

(13) Hu, S.; Wan, C.; Li, Y. Production and characterization of biopolyols and polyurethane foams from crude glycerol based liquefaction of soybean straw. *Bioresour. Technol.* **2012**, *103* (1), 227−233.

(14) Verdolotti, L.; Lavorgna, M.; Lamanna, R.; Di Maio, E.; Salvatore, S. Polyurethane-silica hybrid foam by sol−gel approach: Chemical and functional properties. *Polymer* **2015**, *56*, 20−28.

(15) Fu, C.; Yang, Z.; Zheng, Z.; Shen, L. Properties of alkoxysilane castor oil synthesized via thiolene and its polyurethane/siloxane hybrid coating films. *Prog. Org. Coat.* **2014**, *77* (8), 1241−1248.

(16) Zhai, L.; Liu, R.; Peng, F.; Zhang, Y.; Zhong, K.; Yuan, J.; Lan, Y. Synthesis and characterization of nanosilica/waterborne polyurethane end-capped by alkoxysilane via a sol-gel process. *J. Appl. Polym. Sci.* **2013**, *128* (3), 1715−1724.

(17) Unkelhäußer, T., Hallack M., Görlitzer H., Lomölder R. The best of two worlds - silane-urethane hybrid crosslinkers create scratch-resistant clearcoats. *European Coatings Journal*; Technical paper − Crosslinkers, 07/08, **2015**; pp 1221−1225.

(18) Mori, R. Inorganic−organic hybrid biodegradable polyurethane resin derived from liquefied Sakura wood. *Wood Sci. Technol.* **2015**, *49* (3), 507−516.

DOI: 10.1021/acssuschemeng.5b00723
ACS Sustainable Chem. Eng. 2015, 3, 2533−2541

(19) Furer, V. L. The IR spectra and hydrogen bonding of toluene-2,6-bis(methyl) and 4,4′-diphenylmethane-bis(methyl)carbamates. *J. Mol. Struct.* **2000**, *520* (1−3), 117−123.
(20) Mishra, A. K.; Chattopadhyay, D. K.; Sreedhar, B.; Raju, K. V. S. N. FT-IR and XPS studies of polyurethane-urea-imide coatings. *Prog. Org. Coat.* **2006**, *55* (3), 231−243.
(21) Jena, K. K.; Chattopadhyay, D. K.; Raju, K. V. S. N. Synthesis and characterization of hyperbranched polyurethane-urea coatings. *Eur. Polym. J.* **2007**, *43* (5), 1825−1837.
(22) Hummel, D. O.; Ellinghorst, G.; Khatchatryan, A.; Stenzenberger, H. D. Segmented co-polyethers with urethane and urea or semi-carbazide links for blood-circulation systems. 2. Infrared-spectroscopic investigations. *Angew. Makromol. Chem.* **1979**, *82* (1), 129−148.
(23) Kurimoto, Y.; Doi, S.; Tamura, Y. Species effects on wood-liquefaction in polyhydric alcohols. *Holzforschung* **1999**, *53* (6), 617−622.
(24) Snyder, R. G.; Hsu, S. L.; Krimm, S. Vibrational spectra in the C H stretching region and the structure of the polymethylene chain. *Spectrochimica Acta Part A: Molecular Spectroscopy* **1978**, *34* (4), 395−406.
(25) Snyder, R. G.; Strauss, H. L.; Elliger, C. A. Carbon-hydrogen stretching modes and the structure of n-alkyl chains. 1. Long, disordered chains. *J. Phys. Chem.* **1982**, *86* (26), 5145−5150.
(26) Parikh, A. N.; Schivley, M. A.; Koo, E.; Seshadri, K.; Aurentz, D.; Mueller, K.; Allara, D. L. n-Alkylsiloxanes: from single monolayers to layered crystals. The formation of crystalline polymers from the hydrolysis of n-octadecyltrichlorosilane. *J. Am. Chem. Soc.* **1997**, *119* (13), 3135−3143.
(27) Bourlinos, A. B.; Chowdhury, S. R.; Jiang, D. D.; An, Y. U.; Zhang, Q.; Archer, L. A.; Giannelis, E. P. Layered organosilicate nanoparticles with liquidlike behavior. *Small* **2005**, *1* (1), 80−82.
(28) Ke, Q.; Li, G.; Liu, Y.; He, T.; Li, X. M. Formation of superhydrophobic polymerized n-octadecylsiloxane nanosheets. *Langmuir* **2009**, *26* (5), 3579−3584.
(29) Lu, Q.; Hao, T.; Ke, Q.; Wang, W.; He, T.; Li, X. M. Morphological control of polymerized n-octadecylsiloxane. *Appl. Surf. Sci.* **2011**, *257* (6), 2080−2085.
(30) Defante, A. P.; Burai, T. N.; Becker, M. L.; Dhinojwala, A. Consequences of Water between Two Hydrophobic Surfaces on Adhesion and Wetting. *Langmuir* **2015**, *31* (8), 2398−2406.
(31) Tyrode, E.; Liljeblad, J. F. Water Structure Next to Ordered and Disordered Hydrophobic Silane Monolayers: A Vibrational Sum Frequency Spectroscopy Study. *J. Phys. Chem. C* **2013**, *117* (4), 1780−1790.
(32) Wang, Y. Y.; Qiu, F. X.; Lv, Y. F.; Xu, J. C.; Yang, D. Y. Preparation and properties of waterborne poly(urethane acrylate)/silica dispersions and hybrid composites. *Plast., Rubber Compos.* **2012**, *41* (10), 418−424.
(33) Lai, X.; Shen, Y.; Wang, L.; Li, Z. Preparation and Performance of Waterborne Polyurethane/Nanosilica Hybrid Materials. *Polym.-Plast. Technol. Eng.* **2011**, *50* (7), 740−747.
(34) Sow, C.; Riedl, B.; Blancjette, P. UV-waterborne polyurethane-acrylate nanocomposite coatings containing alumina and silica nanoparticles for wood: mechanical, optical, and thermal properties assessment. *Journal of Coating Technology and Resins* **2011**, *8* (2), 211−221.
(35) Kabra, A. P.; Mahanwar, P.; Shertukde, V.; Bambole, V. Performance of nanosilica in acrylic polyol 2K polyurethane coatings. *Pigm. Resin Technol.* **2012**, *41* (4), 230−239.
(36) Ugovsek, A.; Sever Škapin, A.; Humar, M.; Sernek, M. Microscopic analysis of the wood bond line using liquefied wood as adhesive. *J. Adhes. Sci. Technol.* **2013**, *27* (11), 1247−1258.
(37) Manifar, T.; Rezaee, A.; Sheikhzadeh, M.; Mittler, S. Formation of uniform self-assembly monolayers by choosing the right solvent: OTS on silicon wafer, a case study. *Appl. Surf. Sci.* **2008**, *254* (15), 4611−4619.
(38) Kurimoto, Y.; Takeda, M.; Doi, S.; Tamura, Y.; Ono, H. Network structures and thermal properties of polyurethane films prepared from liquefied wood. *Bioresour. Technol.* **2001**, *77* (1), 33−40.
(39) Wei, Y.; Cheng, F.; Li, H.; Yu, J. Synthesis and properties of polyurethane resins based on liquefied wood. *J. Appl. Polym. Sci.* **2004**, *92* (1), 351−356.
(40) Kulkarni, S. A.; Mirji, S. A.; Mandale, A. B.; Vijayamohanan, K. P. Thermal stability of self-assembled octadecyltrichlorosilane monolayers on planar and curved silica surfaces. *Thin Solid Films* **2006**, *496* (2), 420−425.
(41) Liu, F.; Wang, S.; Zhang, M.; Ma, M.; Wang, C.; Li, J. Improvement of mechanical robustness of the superhydrophobic wood surface by coating PVA/SiO_2 composite polymer. *Appl. Surf. Sci.* **2013**, *280*, 686−692.
(42) Liu, F.; Gao, Z.; Zang, D.; Wang, C.; Li, J. Mechanical stability of superhydrophobic epoxy/silica coating for better water resistance of wood. *Holzforschung* **2015**, *69* (3), 367−374.
(43) de Meijer, M.; Thurich, K.; Militz, H. Quantitative measurements of capillary coating penetration in relation to wood and coating properties. *European Journal of Wood and Wood Products* **2001**, *59* (1), 35−45.
(44) EN ISO 1522. *Paints and varnishes - Pendulum damping test (ISO 1522:2006)*; European Committee for Standardization: Brussels, 2006.
(45) EN ISO 1518. *Paints and varnishes - Scratch test (ISO 1518:1992)*; European Committee for Standardization: Brussels, 2000.
(46) EN ISO 4624. *Paints and varnishes - Pull off test for adhesion (ISO 4624:2002)*; European Committee for Standardization: Brussels, 2003.
(47) EN 12720. *Furniture-Assessment of surface resistance to cold liquids*; European Committee for Standardization: Brussels, 2009.

NOTE ADDED AFTER ASAP PUBLICATION

This article published September 23, 2015 with an incorrect Figure 1. The correct figure published September 24, 2015.

DOI: 10.1021/acssuschemeng.5b00723
ACS Sustainable Chem. Eng. 2015, 3, 2533−2541